Giant, 16, 2023, 100203

Full-length article

Designing Antifreezing Hydrogels with Enhanced Mechanical Properties Using a Simple Crosslinker

Dong Zhang, Yonglan Liu, William Gross, Yijing Tang, Jie Zheng*

Department of Chemical, Biomolecular, and Corrosion Engineering, The University of Akron, Ohio, USA

Keywords: Hydrogel, Antifreezing, Water state, Water-polymer interaction, Molecular dynamics

Antifreezing hydrogels are essential for materials design and practical applications, but their development and understanding have been challenging due to their high-water content. Current antifreezing hydrogels typically rely on organic solvents or the addition of antifreezing agents. In this study, we present a novel crosslinking strategy to fabricate antifreezing hydrogels without the need for additional antifreezing agents. We introduce a new crosslinker, PEG_n-EGINA, which combines highly hydrophilic EGINA with polyethylene glycol (PEG) of varying molecular weights. Utilizing PEG_n-EGINA as the crosslinker, we synthesize Agar/Polyacrylamide (Agar/PAAm) double-network hydrogels, alongside conventional MBAA-crosslinked hydrogels for comparison. The resulting PEG_n-EGINA-crosslinked hydrogels exhibit inherent antifreezing properties and retain their mechanical integrity even at subzero temperatures for extended periods. Molecular dynamics (MD) simulations further reveal that the antifreezing behavior observed in the PEG_n-EGINA-crosslinked hydrogels can be attributed to their highly hydrophilic and tightly crosslinked double-network structures. These structures enable strong bindings between water and the hydrogel network, thus effectively preventing the formation of ice crystals within the hydrogels. Notably, PEG_n-EGINA-crosslinked hydrogels not only demonstrate superior mechanical performance compared to MBAA-crosslinked hydrogels, but also maintain their mechanical properties even in frozen conditions, making them suitable for a wide range of applications. This study presents a simple yet effective design concept for highlighting the role of novel crosslinker in enhancing antifreezing and mechanical properties, showcasing their potential for various applications that require both antifreezing capabilities and robust mechanical performance.

Introduction

Hydrogels are hydrophilic polymer networks crosslinked and dispersed in water. With their high water content ranging from 50% to 95%, these flexible polymer networks exhibit a unique combination of liquid-like transport behavior and solid-like mechanical properties, making hydrogels highly versatile for a wide range of applications, including soft robotics, flexible electronics, human-machine interfaces, and biomimetic tissues [1-7]. However, despite their numerous advantages, high water content in hydrogels can lead to weak mechanical properties, especially at temperature below the freezing point of water (0 °C)

* Corresponding author.
E-mail address: zhengj@uakron.edu (J. Zheng).

Received 7 September 2023; Received in revised form 23 October 2023; Accepted 26 October 2023

https://doi.org/10.1016/j.giant.2023.100203

[8]. Under subzero temperatures, hydrogels tend to freeze water into ice crystals, rendering them mechanically fragile and causing a loss in their exceptional properties, including conductivity, transparency, elasticity, and flexibility [9-11]. Therefore, there is a pressing need to develop anti-freezing hydrogels capable of functioning across a wide temperature range.

Conventional strategies for fabricating antifreezing hydrogels involve incorporating antifreezing agents (*e.g.*, salts, organic solvents, charged nanofillers) into hydrogel matrix, which leads to the development of two main categories of antifreezing hydrogels: ionic hydrogels and organohydrogels with frozen tolerance property [12-14]. Extensive efforts have been made to develop numerous ionic antifreezing hydrogels, including Polyacrylamide/alginate-$CaCl_2$ ionic hydrogels [15], poly(acrylamide-*N*-acryloyl-2-glycine)-ions hydrogels [16], poly(AAm-*co*-VI)/QCS-Fe^{3+} ionic hydrogels [17], PDA-rGO/SA/PAAm-Ca^{+2} hydrogels [18], graphene/PEDOT:PSS hydrogel [19], PVA-TA-NaCl-ionic liquid hydrogels [20], poly(acrylamide-*co*-2-hydroxyethyl acrylate)/ionic liquid hydrogels [21], Ca-alginate/polyacrylamide-NH_4Cl hydrogels [22], $ZnCl_2$/$CaCl_2$-cellulose hydrogels [23]. These hydrogels are typically fabricated using relatively simple strategies, such as post-immersion of ions/salts into pre-prepared hydrogels or direct utilization of ions as crosslinkers during the gelation process. By incorporating common ions or salts (such as $CaCl_2$, NaCl, KCl, $MgCl_2$, $ZnCl_2$), these ions/salts hinder or disrupt the formation of ice crystals and effectively lower the freezing point of the hydrogels, thus enabling the hydrogels to maintain its fluidity at subzero temperatures.

On the other hand, organohydrogels, such as polyacrylamide/montmorillonite/carbon nanotube organohydrogels [24], ethylene glycol/glycerol organohydrogels [25], utilize organic solvents, such as dimethyl sulfoxide (DMSO), ethanol, or glycerol, as cryoprotectants or crosslinking agents within the hydrogel matrix. These organic solvents play a crucial role in lowering the freezing point of the hydrogel and protecting it from ice crystal formation. However, due to the inherent incompatibility between organic solvents and hydrophilic polymers, not all organic solvents can effectively initiate the gelation process with the desired hydrophilic polymers. Thus, fabricating organohydrogels requires careful selection of suitable organic solvents, precise control of polymer-solvent interactions, and optimization of gelation conditions for achieving successful gelation. Moreover, there is an alternative approach to incorporate Antifreeze proteins (AFPs) into hydrogels to enhance their antifreezing properties. However, in such cases, the overall effectiveness of AFPs in preventing freezing may not reach an optimal level. This could be due to AFPs experiencing structural misfolding within the polymer matrix, resulting in the loss of their antifreezing function. In simpler terms, merely adding AFPs to conventional hydrogels does not necessarily confer effective antifreezing properties. Although there have been a limited number of studies successfully integrating AFPs into antifreezing hydrogels, such as AFPs-PAM/PVA [26] and AA/ISP-Ca [27], it remains a considerable challenge to design protein-based antifreezing hydrogels with a well-defined antifreezing mechanism.

In both types of antifreezing hydrogels, the incorporation of antifreezing agents (ions, salts, organic solvents) modifies the water structure, dynamics, and interactions within the hydrogel matrix, thereby altering the phase diagram of water. These modifications are anticipated to inhibit the formation of ice crystals while retaining the inherent properties of the hydrogels, even under subzero temperatures [9], [28]. However, the incorporation of antifreezing agents can lead to the formation of heterogeneous network structures within the hydrogels, which may compromise their mechanical properties during deformation or freezing processes [2]. Another challenge in materials design is the lack of a new design strategy for fabricating antifreezing hydrogels that can maintain their mechanical properties under subzero temperatures and during deformation.

We recently demonstrated a simple and robust crosslinking strategy to fabricate a family of a 4, 9-dioxo-5, 8-dioxa-3, 10-diazadodecane-1, 12-diyl diacrylate (EGINA)-crosslinked double-network hydrogels without adding any antifreezing additives [29]. These hydrogels exhibit intrinsic, built-in antifreezing properties and maintain their mechanical properties at -20°C for hours. In order to further advance this crosslinking design concept for antifreezing hydrogels, we first synthesized new highly hydrophilic reactive crosslinkers by combining EGINA with polyethylene glycol (PEG) of different OEG segment lengths, i.e., EGINA, PEG_n-EGINA (n=200, 400 g/mol) (Figure 1a), and then used these crosslinkers to crosslink Agar/Polyacrylamide (Agar/PAAm) double networks by a one-pot method [30]. For comparison purposes, we also utilized a conventional crosslinker, methylene-bis-acrylamide (MBAA), to crosslink Agar/PAAm double network hydrogels. This allowed us to assess and compare the antifreezing and mechanical properties of the MBAA-crosslinked hydrogels with those of the PEG_n-EGINA-crosslinked Agar/PAAm hydrogels. Overall, this study introduces a simple yet effective design concept for antifreezing hydrogels, highlighting the role of the novel crosslinker in enhancing their mechanical properties. The results emphasize the potential of PEG_n-EGINA-crosslinked hydrogels for applications that require both antifreezing capabilities and robust mechanical performance. This work contributes to the advancement of antifreezing materials design and provides valuable insights into the behavior of hydrogels in subzero environments.

Results and Discussion

Design and Synthesis of PEGn-EGINA crosslinker and PEGn-EGINA-crosslinked Agar/PAAm Double-Network Hydrogels

We first synthesized a crosslinker derived from PEG and INA through a one-step additive reaction, which was confirmed by ^{1}H-NMR spectrum (Figure 1b). Both PEG and ethylene glycol (EG) possess structures similar to alcohol-like molecules, which provide abundant hydrogen bonding receptor/donor sites (O-, NH-, COO-) for strongly interacting with water molecules to form a robust hydrogen bond network. Furthermore, the symmetrical double bonds present in PEG_n-EGINA allow for chemical crosslinking with polymer chains, leading to the formation of stable and cohesive networks. It is important to note that when investigated using Differential Scanning Calorimetry (DSC) in Figure 1c, EGINA and PEG_{200}-EGINA crosslinkers exhibit negligible transition temperatures from liquid to solid states in comparison to EG and PEG_{400}-EGINA. The

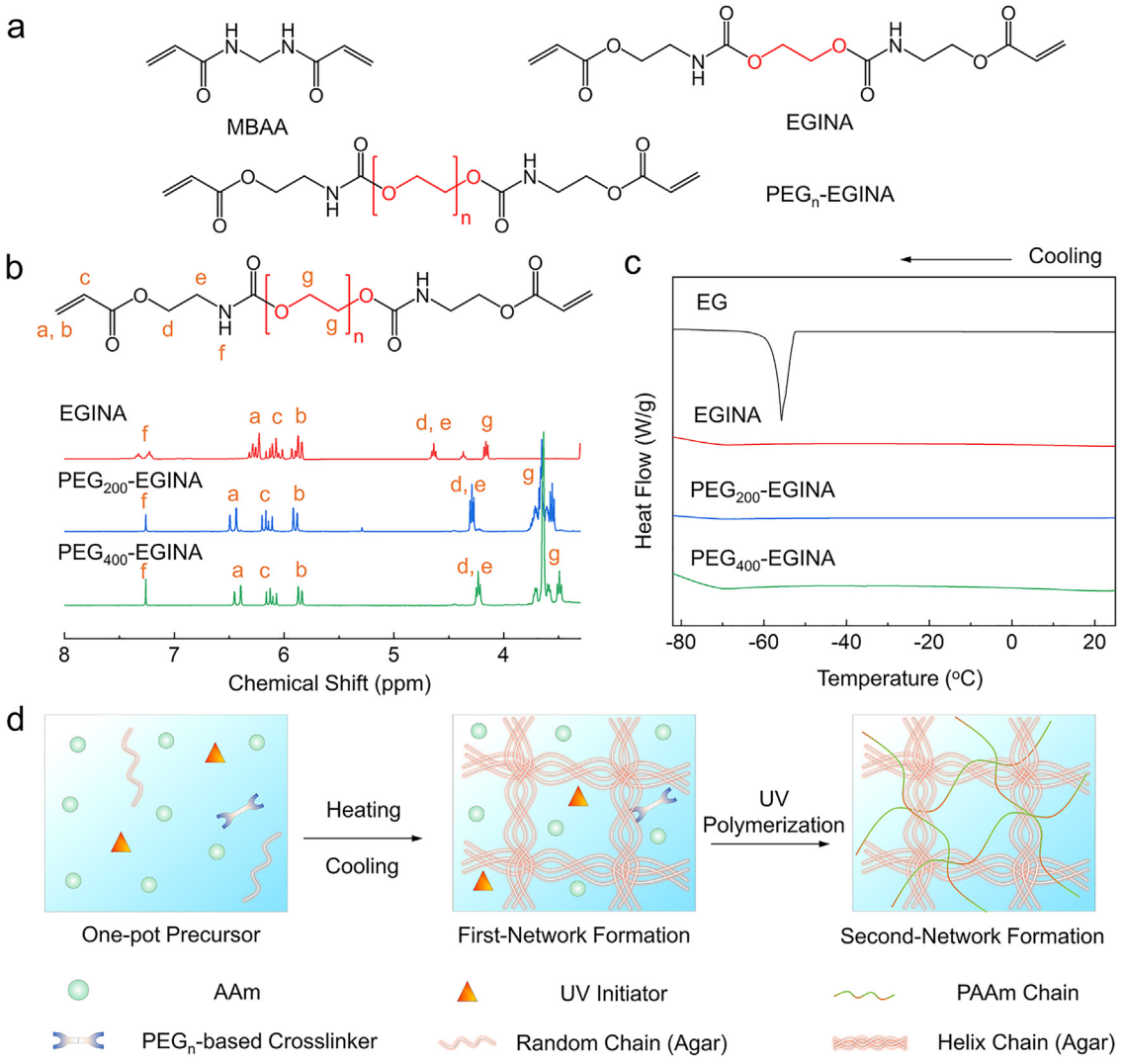

Figure 1

Synthesis and characterization of PEGn-EGINA crosslinker and its crosslinked Agar/PAAm DN hydrogels. (a) Chemical structure of MBAA, EGINA, and PEGn-EGINA crosslinkers. n=200 and 400 g/mol. (b) 1H-NMR spectra of EGINA, PEG200-EGINA, and PEG400-EGINA. (c) DSC curves of EG, EGINA, PEG200-EGINA, and PEG400-EGINA. (d) One-pot synthesis procedure of Agar/PAAm DN hydrogels crosslinked by PEGn-EGINA, EGINA, or MBAA.

transition temperature for PEG$_{400}$-EGINA is -77°C, while the common antifreeze EG showed higher freezing temperature of -58°C. The structural design of the PEG$_n$-EGINA crosslinker enables strong interactions with polymer networks and water molecules through hydrogen bonding, facilitates polymer chain clustering around the crosslinker sites, and controls the spacing between adjacent polymer chains. All these effects collectively promote the formation of tightly bound water with polymers and crosslinkers, leading to a reduction in free water molecules within the hydrogels and preventing the formation of ice crystals. Consequently, these effects are expected to contribute to the antifreezing properties of the PEG$_n$-EGINA-crosslinked hydrogels. Molecular simulations revealed that the PEG$_n$-EGINA molecule has more than twice the number of hydrogen bonding sites compared to the conventional crosslinker MBAA, while maintaining a similar degree of unsaturation (carbon-carbon double bonds) and hydrophilic factor.

To investigate the crosslinking effects of PEG$_n$-EGINA and MBAA, we conducted a gelation study on Agar/PAAm DN hydrogels as a proof-of-concept [31]. Briefly, in a single water pot, all reactants including agar, AAm monomers, UV-initiators, and chemical cross-linker were mixed to synthesize DN hydrogels through a heating-cooling-photopolymerization process [29-30]. The agarose, a major gel fraction in agar, was dissolved at temperatures higher than its melting point (90~95°C), resulting in the formation of linear macromolecules and a transparent, low-viscosity solution. The solution was then gradually cooled to room temperature, allowing the agar to form the first-network gel through physical linkage by agar helix bundles. Subsequently, upon photo-initiation, the second network of PAAm gel was crosslinked using either PEG$_n$-EGINA or MBAA, resulting in the successful synthesis of PEG$_n$-EGINA- or MBAA-crosslinked Agar/PAAm DN gels (Figure 1d). The entire gelation process took approximately 1-2 hours, followed by the

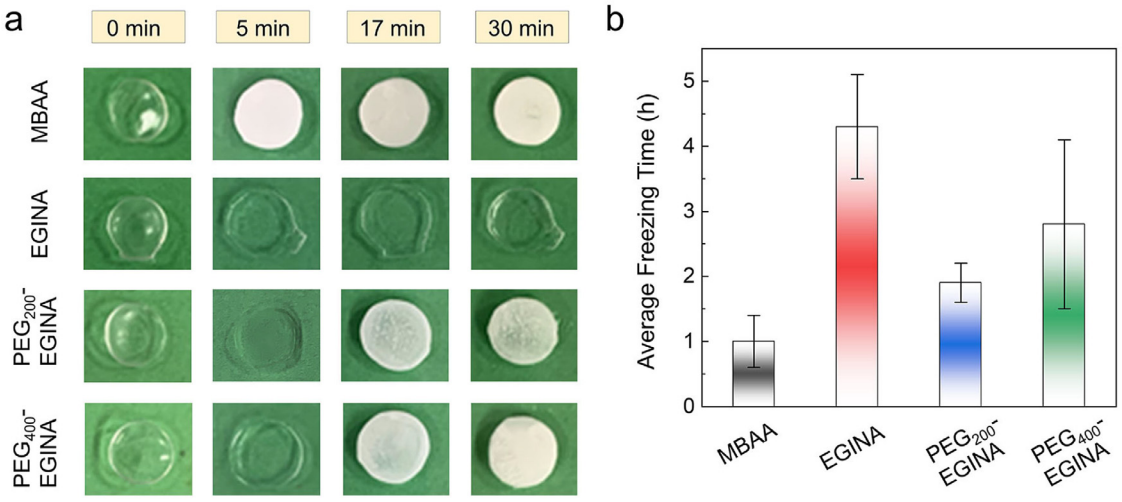

Figure 2

Evaluation of the antifreezing performance of PEGn-EGINA-crosslinked hydrogels. (a) Visual inspection of the antifreezing behavior of MBAA- and PEGn-EGINA-crosslinked Agar/PAAm hydrogels at -20°C for 0, 5, 17, and 30 minutes. (b) Average freezing times of Agar/PAAm DN hydrogels with four different crosslinkers at -20°C.

removal of excess unreacted precursors through rinsing with DI water.

Antifreezing Performance of PEGn-EGINA-crosslinked Agar/PAAm Hydrogels

To facilitate further discussion, we designated the Agar/PAAm DN hydrogels crosslinked with PEG_n-EGINA as PEG_n-EGINA-hydrogels, where the variable n represents the average molecular weight of PEG chains within the crosslinker. Figure 2a illustrates the time-dependent images of Agar/PAAm gels crosslinked with PEG_{200}-EGINA, PEG_{400}-EGINA, EGINA, and MBAA at -20°C. At the beginning of the freezing experiment (0 min), all original hydrogels exhibited a visually clear and transparent appearance, reflecting their soft and wet nature. After 5 min of freezing, only the MBAA-crosslinked gels began to exhibit the formation of ice crystals on their surfaces, while EGINA- and PEG_n-EGINA-crosslinked gels still retained their original transparent and soft appearance. MBAA gels were almost completely frozen with a rigid shape after 10-min freezing, while PEG_{200}-EGINA and PEG_{400}-EGINA gels began to develop a very thin layer of white ice (squeezed from the crosslinked networks) on the top surface, but the entire gels maintained their structural flexibility and could be bent without any signs of breakage. After 17 min, the MBAA gels were fully frozen, exhibiting a solid and rigid state. In contrast, the PEG_n-EGINA gels remained almost unchanged in terms of their appearance and mechanical flexibility. They could still be bent, twisted, and compressed without any noticeable alterations. After 30 min, both PEG_{200}-EGINA and PEG_{400}-EGINA gels experienced an increase in stiffness, but they remained bendable. Additionally, the frozen layers on their surfaces became thicker. Among the four types of gels, EGINA gels demonstrated superior tolerance to freezing and maintained their transparent and soft nature throughout the entire 30-min freezing period at -20°C. Further analysis of freezing time for multiple samples of the same gels, as illustrated in Figure 2b, revealed a decrease order of freezing time: EGINA (4.3 h) > PEG_{400}-EGINA (2.8 h) > PEG_{200}-EGINA (1.9 h) > MBAA (1 h). Evidently, regardless of the network compositions, all of EGINA-crosslinked DN hydrogels took longer time to achieve a completely frozen state from their initial state than MBAA-crosslinked hydrogels. Furthermore, an increase in the number of PEG repeated units in the crosslinker resulted in longer freezing times and improved antifreezing properties of the hydrogels. Additionally, within the same hydrogel systems, a lower water content contributed to a longer antifreezing time.

To obtain a more accurate understanding of the frozen state within the hydrogels, thermal infrared (IR) images were captured to analyze the *in-situ* temperature distribution of various crosslinked hydrogels during both the freezing and thawing processes (Figure 3). This allowed for a detailed characterization of the temperature changes within the hydrogel samples. During the freezing process, as the temperature was cooled from room temperature to -60°C, the EGINA-crosslinked hydrogels maintained their original temperature distribution nearly unchanged over time. This observation highlighted their high resistance to freezing, in sharp contrast to the rapid melting process observed in MBAA-crosslinked hydrogels (Figure 3a). A similar temperature distribution pattern was observed during the warming process from 0 to 25°C for both EGINA- and MBAA-crosslinked hydrogels, i.e., MBAA-crosslinked hydrogels thawed much faster than EGINA-crosslinked hydrogels (Figure 3b). These findings suggest that the relatively stable temperature gradients in EGINA-crosslinked DN hydrogels create additional free energy barriers that hinder ice nucleation. These findings provide further confirmation that the remarkable antifreezing property observed in PEG_n-EGINA hydrogels can be attributed to two main factors. Firstly, the PEG_n-EGINA crosslinkers, which combine PEG and EGINA motifs, exhibit strong water-binding properties. Secondly, the presence of tightly crosslinked and highly interpenetrating DN structures allows for the imposition of robust compositional and spatial effects, leading to enhanced

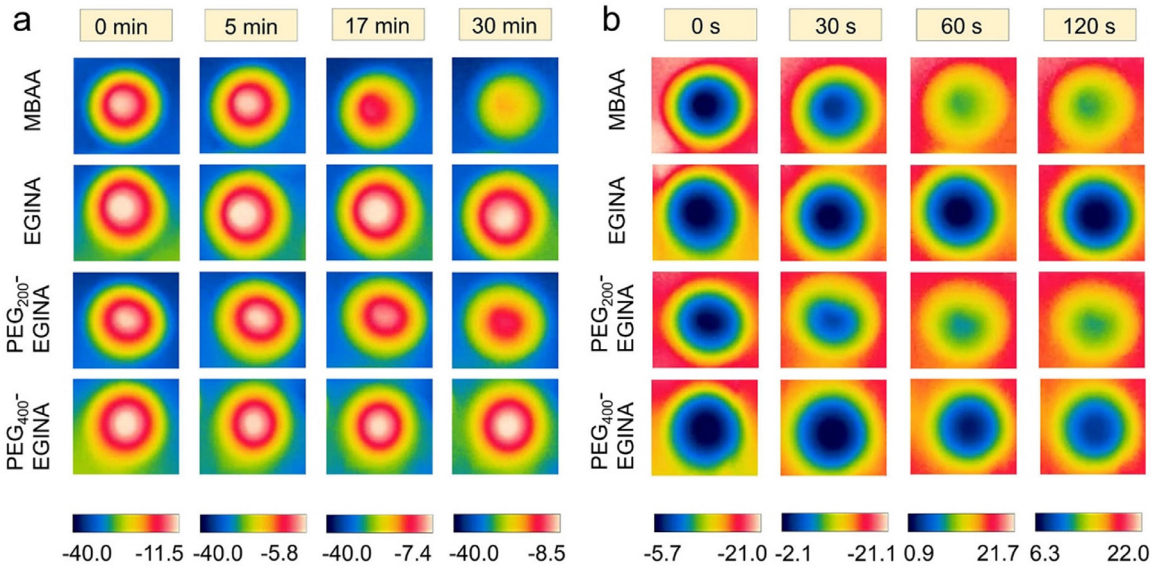

Figure 3

In-situ temperature distribution for Agar/PAAm hydrogels crosslinked by MBAA, EGINA, and PEGn-EGINA during the (a) freezing and (b) thawing processes by an IR camera. Supplementary Materials include movies S1 and S2 illustrating these freezing and thawing processes. Temperature measurements are in°C.

polymer-water interactions facilitated by hydrogen bonding and an increased number of tightly bound water molecules. These enhanced polymer-water interactions effectively suppress ice nucleation, accumulation, and growth. As a result, EGINA plays a crucial role in significantly reducing the freezing point of all tested DN hydrogels, regardless of their specific network compositions. From a structural design standpoint of antifreezing crosslinkers, the crucial factors include providing an appropriate balance of chain flexibility and incorporating hydrogen bond acceptors and donors along the polymer chains. Excessive or redundant ethylene oxide (EO) segments can introduce hydrophobicity, potentially weakening the interactions between water and crosslinkers, thereby compromising their ability to resist freezing. This trend was confirmed by our experimental data during the design phase. For instance, within the hydrogels, PEG_{400}-EGINA exhibited lower antifreezing capacity compared to both EGINA and PEG_{200}-EGINA. Furthermore, the antifreezing properties can be further tailored by modifying PEG chains with various active functional groups (e.g., hydroxyl (-OH), amino (-NH2), carboxyl (-COOH), and maleimide groups) within the hydrogel network.

Mechanical Performance of PEGn-EGINA-crosslinked Agar/PAAm Hydrogels at Subzero Temperatures

We further examined the mechanical properties of PEG_{200}-EGINA, PEG_{400}-EGINA, EGINA- and MBAA-crosslinked DN hydrogels prepared at both -20°C and room temperature using tensile and compression tests (Figure 4). Notably, all the tensile and compression tests were performed at room temperature, where the frozen hydrogels were simultaneously subjected to both deformation and thawing processes. Prior to conducting any mechanical tests, it was observed that the as-prepared frozen gels at -20°C exhibited distinct differences. The EGINA-crosslinked DN hydrogels remained soft and deformable, allowing for repeated stretching and bending. In contrast, the MBAA-crosslinked DN hydrogels became excessively rigid and brittle, unable to sustain any mechanical deformation. Next, tensile stress–strain curves of different crosslinked Agar/PAAm hydrogels, as illustrated in Figure 4a-b, showed that MBAA-crosslinked hydrogels displayed the highest tensile properties due to the higher crosslinking efficiency to withstand larger tensile forces without breaking or deforming at room temperature. Their tensile strength and elongation dramatically decreased from 0.65 MPa and 2200% at room temperature to 0.34 MPa and 253% at -20°C, respectively, indicating enhanced network fragility after water freezing in binary polymeric system. Comparatively, EGINA-crosslinked hydrogels exhibited intermediate tensile properties between the PEG_n-EGINA- and MBAA-crosslinked hydrogels. Interestingly, the frozen EGINA hydrogels (tensile strength of 0.35 MPa, tensile strain of 609%, elastic modulus of 0.43 MPa) demonstrated even better tensile properties than as-prepared ones at room temperature (tensile strength of 0.25 MPa, tensile strain of 503%, elastic modulus of 0.32 MPa). The tensile properties of PEG_n-EGINA-crosslinked hydrogels were further enhanced by both the presence of the crosslinker and the frozen state. PEG_{200}-EGINA hydrogels exhibited an increase in tensile strength and tensile strain from 0.25 MPa and 503% at room temperature to 0.36 MPa and 563% at -20°C, respectively. Similarly, PEG_{400}-EGINA hydrogels demonstrated an increase in tensile strength and tensile strain from 0.15 MPa and 200% at room temperature to 0.22 MPa and 295% at -20°C. Interestingly, both frozen PEG_n-EGINA-crosslinked hydrogels displayed a distinct yielding point at the onset of stretching, a feature that was absent in the as-prepared hydrogels at room temperature. The presence of a yielding point in the frozen PEG_n-EGINA-crosslinked hydrogels can be attributed to the enhanced water-polymer interactions, particularly the strengthened hydrogen bonds between water molecules and the polymer network. When the hydrogels are subjected to subzero temperature, the formation of ice crystals allows for increased

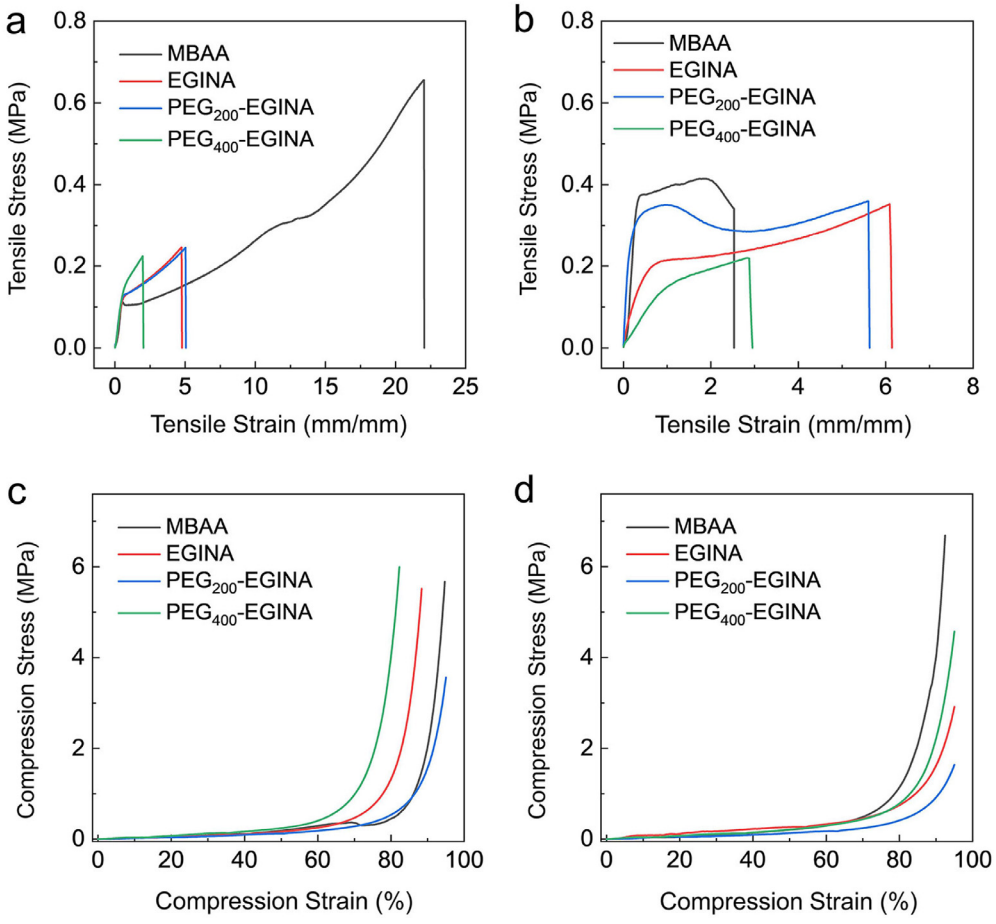

Figure 4

Comparative mechanical properties of Agar/PAM hydrogels crosslinked by MBAA, EGINA, and PEGn-EGINA at (a, c) room temperature and (b, d) -20°C, evaluated by (a-b) tensile tests and (c-d) compressive tests.

interaction between water molecules and the polymer chains. This enhanced water-polymer interaction results in a more robust and cooperative response to external forces, leading to the observed yielding point during stretching. In contrast, the as-prepared hydrogels at room temperature do not experience the same level of enhanced hydrogen bonding due to the absence of freezing, resulting in the absence of a yielding point.

Concurrently, Figure 4c-d illustrates the compression results, showing the soft and compressible nature of MBAA hydrogels at room temperature. As the temperature decreased to -20°C, there was a slight reduction in their compressive strength, with values decreasing from 5.8 to 6.7 MPa. Simultaneously, an increase in the average compressive Young's modulus was observed within the 60-80% strain range, measuring 4.3 MPa. This enhancement can be attributed to the strengthening of the frozen networks. Nevertheless, as the compression process continued, the unavoidable melting of ice crystals prevented a significant further increase in the ultimate compressive strength. In contrast, the three EGINA-crosslinked hydrogels displayed higher compressive strength, ranging from 3.5-6.0 MPa at room temperature. Interestingly, all as-prepared hydrogels exhibited higher compressive strength than the frozen hydrogels, presumably due to the rigidity of the polymer network. During the freezing process, the formation of ice crystals can introduce rigidity into the hydrogel structure. This rigidity can hinder the compressive deformation of the hydrogel, resulting in a lower compressive strength. On the other hand, the as-prepared EGINA-crosslinked hydrogels do not undergo the freezing process, allowing them to retain their inherent flexibility and deformability. As a result, the as-prepared hydrogels exhibit higher compressive strength due to their ability to undergo larger compressive deformations without significant resistance. Overall, the enhanced mechanical properties, specifically the stretchability, of EGINA-crosslinked hydrogels are likely derived from the non-frozen elasticity of the polymer network. In contrast, the MBAA-crosslinked hydrogels develop rigid and brittle networks as a result of the formation of ice crystals at subzero temperatures. These ice crystals contribute to the stiffening of the crosslinked polymeric gels. However, despite the stiffening effect, the frozen hydrogels still exhibit a certain degree of deformability, similar to the toughening observed in nanocomposite hydrogels.

As always, the concentration of the crosslinker indeed plays a significant role in determining the mechanical properties of soft hydrogels. In typical covalent chemical crosslinking systems, even a very low concentration (0.1-0.5 wt.%) of crosslinkers,

such as MBAA, can result in soft hydrogels with favorable mechanical properties. However, as the concentration increases, it progressively enhances brittleness and renders the hydrogels more susceptible to fracturing under slight deformation. This phenomenon occurs because higher crosslinker concentrations effectively reduce the length of the polymer chains within the hydrogel network. However, it would be a different scenario how crosslinker content affects antifreezing properties. Antifreezing property is driven by the microscopic formation and propagation of ice across polymer networks within the hydrogels, occurring predominantly at the curved interface between the EGINA-crosslinked chains. Given the pronounced hydrophilicity of EGINA crosslinkers, their crosslinked polymer chains enable long-range interactions that affect water dynamics within the network through weakening the favorable thermodynamics to generate a hexagonal pattern (ice crystals). At lower concentrations (<0.1 wt.%), PEGn-EGINA crosslinked hydrogels exhibit significantly enhanced antifreezing capabilities. However, such improved antifreezing properties would be saturated rapidly as crosslinker concentration is approach to a threshold value, because the size of crosslinking network cannot be continuously reduced. From a scientific standpoint, the content of PEGn-EGINA crosslinkers impacts both the mechanical and antifreezing attributes of the hydrogels. Nonetheless, these attributes display asynchronous adjustments due to their distinct operational ranges.

Molecular Simulations of PEG_n-EGINA-crosslinked Agar/PAAm Hydrogels at Subzero Temperatures

We recently developed a "random walk reactive polymerization" (RWRP), which mimics the process of radical polymerization and allows us to create physically-chemically linked Agar/PAAm DN hydrogels using monomers and different crosslinkers [32]. To further gain insights into the antifreezing properties of these hydrogels, here we employed molecular dynamics (MD) simulations to investigate the structure, dynamics, and interactions between the polymer networks and water molecules at temperatures of -20°C and 25°C. Figure 5a shows an initial atomic structure of an Agar/PAAm DN hydrogel. This structure comprises two distinct networks: the first agar network (van der Waals balls in black color) consists of preformed α-helical bundles, within which a high density of hydrogen bonding offers a strong associative force for the assembly of three agar helices together. The second PAAm network (small ball-stick presentation with light grey color) densely packs around the first agar network. This arrangement demonstrates an interpenetrating network structure, reflecting the organization and interaction between the two polymer networks within the hydrogel.

To investigate the influence of temperature on polymer chain mobility, we examined the root-mean-square fluctuation (RMSF) of atomic positions in MBAA- and PEG_n-EGINA-crosslinked Agar/PAAm hydrogels at -20°C and 25°C, as shown in Figure 5b. An initial observation reveals that the PEG_n-EGINA-crosslinked Agar/PAAm networks (RMSF values: 4.47-4.8 Å) consistently displayed higher mobility than the MBAA-crosslinked networks (RMSF values: 2.52-4.11 Å), regardless of temperature. This discrepancy in network mobility can be attributed to the distinct characteristics of the crosslinkers employed. Moreover, as the temperature decreased from 25 to -20°C, both hydrogels exhibited a decrease in their RMSF values. The RMSF values for MBAA-crosslinked networks reduced from 4.11 Å to 2.52 Å, while for PEG_n-EGINA-crosslinked networks, the values decreased from 4.8 Å to 4.47 Å. Interestingly, the mobility of MBAA-crosslinked networks displayed higher sensitivity to temperature changes, as compared to the minimal change observed in the mobility of PEG_n-EGINA-crosslinked networks. This discrepancy reflects the superior antifreezing property of PEG_n-EGINA-crosslinked hydrogels. The decrease in overall network mobility at lower temperatures can primarily be attributed to the reduction in molecular motion of the polymer chains and changes in solvation properties within the hydrogels. As the temperature decreases, the thermal energy available for the molecular motion of both polymer chains and water molecules decreases. This decrease in thermal energy results in reduced polymer chain flexibility and mobility. Additionally, the conformational restriction at lower temperatures leads to enhanced interactions between polymer chains and water molecules, due to increased proximity and reduced solvation effects. These enhanced interactions further restrict the mobility of the networks, contributing to the overall decrease in network mobility at lower temperatures.

To further investigate the influence of crosslinkers on the antifreezing property of Agar/PAAm hydrogels, we calculated the total number of hydrogen bonds between water molecules and polymer chains from 100-ns MD simulations. Considering that Agar, PAM, and the crosslinkers contain various hydrophilic groups such as OH-, NH-, and O=, we observed a consistent and stable hydrogen bond network between the polymers and water molecules in both MBAA- and PEG_n-EGINA-crosslinked hydrogels, irrespective of their network components and temperatures. In Figure 5c both hydrogels at -20°C exhibited a higher number of hydrogen bonds with polymers compared to the same hydrogels at 25°C. The MBAA-crosslinked hydrogels had an average of 6730 hydrogen bonds at -20°C and 5546 hydrogen bonds at 25°C, while the PEG_n-EGINA-crosslinked hydrogels had an average of 7240 hydrogen bonds at -20°C and 7011 hydrogen bonds at 25°C. The decrease in temperature results in a decrease in molecular mobility, leading to an increased attraction of free water molecules to the polymer chains. This enhanced attraction promotes the formation of hydrogen bonds between the polymer chains and water molecules, causing a shift from a state of free water to polymer-bound water molecules. Additionally, the reduced thermal energy at lower temperatures further strengthens the stability of these hydrogen bonds between the water molecules and hydrophilic polymers. These computational findings align with recent spectroscopy measurements, where hydrogen bonds become disrupted at higher temperatures [33]. Furthermore, PEG_n-EGINA-crosslinked networks displayed a higher number of hydrogen bonds with water molecules compared to MBAA-crosslinked networks, due to the presence of hydrophilic groups in PEG_n-EGINA. These hydrophilic groups, such as OH-, NH-, and O=, have a greater affinity for water molecules, promoting stronger interactions and facilitating the formation of hydrogen bonds. Consequently, these interactions contribute to the enhanced antifreezing property of the PEG_n-EGINA-crosslinked hydrogels, as they provide additional stability and

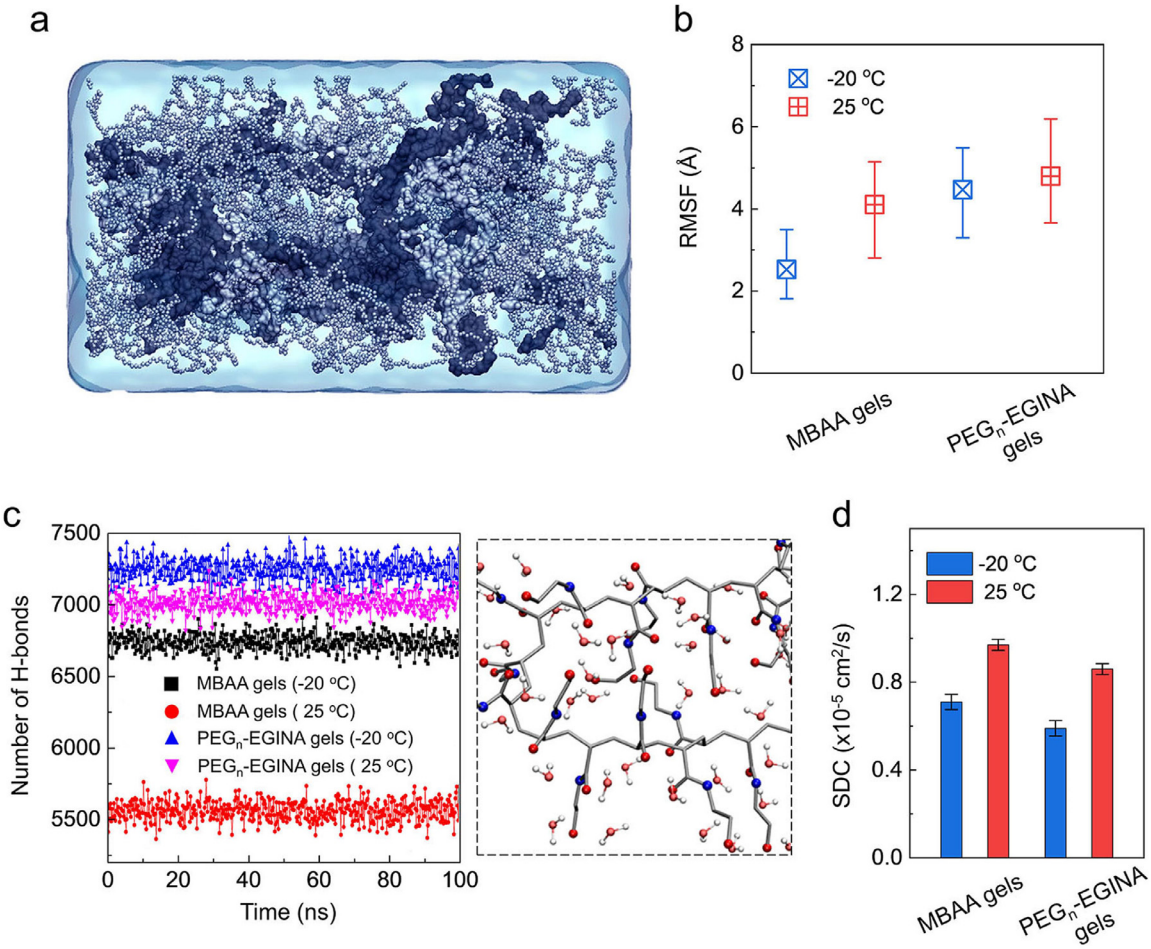

Figure 5

Molecule dynamics simulations of different crosslinked Agar/PAAm hydrogels at temperatures of -20°C and 25°C. (a) Initial atomic structure of Agar/PAAm hydrogels consisting of the first Agar network by co-assembling α-helical agar bundles (van der Waals balls in black color), the second PAAm network (small ball-stick presentation with light grey color), and water molecule (transparent blue background). (b) Root-mean-square-fluctuations (RMSFs), (c) Time-dependent of hydrogen bonds between polymers and water molecules, and (d) Self-diffusion coefficient of water molecules around polymer chains for MBAA- and PEGn-EGINA-crosslinked Agar/PAAm hydrogels at -20°C and 25°C. RMSF values in (b) are calculated based on the carbon atoms in the backbone of the two networks, while a representative MD snapshot in (c) illustrates hydrogen bonds formed between water molecules and PEGn-EGINA networks.

contribute to the retention of water molecules within the network structure.

From a dynamic perspective of water molecules surrounding polymer networks in hydrogels, we determined the self-diffusion coefficients (SDCs) of water molecules in proximity to polymer chains. In Figure 5d, the SDCs of water molecules in all hydrogels (0.59-0.97 $\times$ 10^{-5} cm^2/s) were significantly smaller than that of bulk water (2.54 $\times$ 10^{-5} cm^2/s), clearly indicating the presence of polymer-water interactions that impede the movement of water within the polymer network. Decreasing the temperature from 25 to -20 °C resulted in reduced SDCs of water molecules in both MBAA-crosslinked hydrogels, from 0.97 $\times$ 10^{-5} to 0.71 $\times$ 10^{-5} cm^2/s, and PEG_n-EGINA-crosslinked hydrogels, from 0.86 $\times$ 10^{-5} to 0.59 $\times$ 10^{-5} cm^2/s. This finding aligns with the expectation that water molecules exhibit increased mobility at higher temperatures. Furthermore, our findings revealed that water molecules in PEG_n-EGINA-crosslinked hydrogels consistently exhibited lower SDC values compared to those in MBAA-crosslinked hydrogels at both temperatures. This observation aligns with our previous findings, indicating stronger interactions between water molecules and PEG_n-EGINA networks.

Conclusions

The development and understanding of antifreezing hydrogels pose significant challenges in materials design and practical applications, primarily due to their high-water content. Current antifreezing hydrogels are mostly limited to either organic/icephobic materials that lack water or hydrophilic hydrogels that require the addition of antifreezing agents. In this study, we address this issue by presenting a straightforward crosslinking strategy for the development of antifreezing hydrogels without the need for additional antifreezing agents. Our approach involves the synthesis of a new crosslinker, PEG_n-EGINA, which combines highly hydrophilic EGINA with polyethylene glycol (PEG) of varying molecular weights (EGINA, PEG_{200}-EGINA, PEG_{400}-EGINA). Using this crosslinker, we successfully fabricated PEG_n-EGINA-crosslinked Agar/Polyacrylamide (Agar/PAAm) double-network hydrogels,

alongside conventional methylene-bis-acrylamide (MBAA) crosslinked Agar/PAAm hydrogels for comparison. Remarkably, the resulting PEG_n-EGINA-crosslinked hydrogels demonstrate inherent antifreezing properties and retain their mechanical properties even at -20°C for prolonged periods. Molecular simulations further elucidate that the general antifreezing property observed in the EGINA-crosslinked hydrogels, irrespective of their specific network compositions, can be attributed to their highly hydrophilic and tightly crosslinked double-network structures. These structures facilitate strong bindings between water and the hydrogel network, effectively preventing the formation of ice crystals from free water within the hydrogel. This work not only presents a simple and impactful design concept for antifreezing hydrogels, but also contributes to a better understanding of the relationship between composite structures, properties, and antifreezing behavior in materials. Furthermore, it provides insights into the fundamental properties of water confinement in wet-soft materials, paving the way for future advancements in the field of antifreezing materials.

Materials and Methods

Materials

Ethylene glycol, polyethylene glycols (PEG_n) with varying molecular weights (200, 400 g/mol), dichloromethane, agar ((>300 g/cm^2 of gel strength, 85-95°C of melting point), acrylamide (AAm), N, N′-methylenebis(acrylamide) (MBAA), and 2-hydroxy-4′-(2-hydroxyethoxy)-2-methylpropiophenone (Irgacure 2959) were purchased from Sigma Aldrich. DI water used in this study was purified by a Millipore water purification system with a resistivity of 18.2 MΩ cm.

Synthesis of antifreezing crosslinkers (PEG_n-EGINA)

Ethylene glycol (EG) and a range of polyethylene glycols (PEG_n) with varying molecular weights (such as 200 and 400 g/mol) were preheated to 110°C, followed by complete dehydration under vacuum (using an oil pump) for a duration of 1.5 h. In a typical synthesis, a solution of 2.8 g of INA in 10 mL of DCM was meticulously added dropwise to the mixture containing 2.0 g of dehydrated PEG_{400} in 30-mL DCM within an ice-salt bath. The reaction mixture was gradually allowed to reach room temperature and was continuously stirred for a span of 3 h. Ultimately, the mixture underwent concentration to dryness under vacuum and was subsequently subjected to purification via column chromatography. This process yielded a transparent liquid with an efficiency exceeding 90%. The elucidation of their chemical structures was accomplished through analysis of their ^{1}H-NMR spectra. All the PEG_n-EGINA crosslinkers were stored in a -20°C freezer.

Preparation of double-network (DN) hydrogels

In a typical one-pot synthesis, 100 mg of agar and 900 mg of AAm, 0.0284 g of photo crosslinker Irgacure 2959 (1 mol% AAm), 59 µL of the fresh prepared MBAA solution (10 mg/mL, 0.03 mol% AAm), and 5 mL of DI water were added into a 20-mL vial, followed by sonication for 15-30 s. Upon sealing the vial, it was then placed within a preheated hot water bath set to 90°C, with magnetic stirring activated. The vial was sealed and placed in a hot water bath preheated to 90°C with magnetic stirring on for 5-10 min until the solution became transparent. Subsequently, the mixture was quickly transferred using the syringe to the glass mold sealed with cling wrap. The mold was permitted to cool naturally at room temperature for a duration of 2-3 hours. This cooling process led to the emergence of a transparent, nearly solid solution, signifying the establishment of the agar network through the sol-gel transition. Subsequently, the mold underwent exposure to an 8 W UV lamp operating at a wavelength of 365 nm. In the case of hydrogel sheets, the duration of UV exposure was set at 1.5 hours, while for cylindrical specimens, a 2-hour UV exposure was administered. Notably, the mold was rotated every 30 minutes during the UV exposure period. To ensure the prevention of any moisture loss prior to conducting experiments, all specimens were hermetically sealed within plastic bags and stored within a refrigerator set to 4°C.

To synthesize the antifreezing PEG_n-EGINA crosslinked hydrogels with desirable mechanical properties, the identical one-pot method was utilized, incorporating a slight modification in the crosslinkers (*i.e.*, EGINA, PEG_{200}-EGINA, and PEG_{400}-EGINA). The quantity of PEG_n-EGINA crosslinkers (10 mg/mL) was fine-tuned to 200 µL, 250 µL, and 300 µL, respectively.

Note: (*i*) All the glass molds, syringe, and stainless needles were preheated in a 70°C oven for at least 5 minutes. (*ii*) Following the designated UV exposure duration, the sheet molds displayed a slender strip of clear solid in proximity to the opening. This occurrence can be attributed to the oxygen inhibition effect inherent in the process of free radical polymerization. It can be mitigated by placing the mold inside a glove box.

Mechanical tests

All mechanical assessments were conducted using an Instron 3345 machine equipped with BlueHill 3 software. The system was calibrated, and the instant strain/ force were zeroed before the measurements. For tensile measurements, the hydrogel specimens were cut using a cutter with the specified dumbbell dimensions (*i.e.*, a width of 3.18 mm, a gauge length of 25 mm, and a thickness of 1.0 mm). Tensile measurements were all performed with a 500 N transducer at the stretching rate of 100 and 400 mm/mm. The tensile strain (ε) was defined as the extension distance ($\triangle L$) divided by the initial length (L_0). Under room temperature testing conditions, the specimen was permitted to regain equilibrium at room temperature for a minimum of 5 minutes after its removal from the 4°C refrigerator, prior to undergoing testing. For subzero testing conditions, each dumbbell specimen was carefully enveloped in cling wrap and then positioned within a -20°C refrigerator for 2 h. Afterward, the specimens were delicately extracted from the freezer using cooled tweezers and promptly inserted into the grips, adhering to the identical testing procedure outlined previously (maintaining the -20°C environment). For compression tests, the specimens were cut from cylindrical syringe molds with a diameter of 10 mm and an average height of 8-10 mm. The compression rate was meticulously regulated at 15 mm/min. Tensile measurements were all performed on a universal Instron 3345 machine with a 500 N transducer at the stretching rate of 100 mm/min.

Note: (*i*) To prevent pre-straining of the specimens, it is recommended to hydrate the grip sections, which facilitates the smooth insertion of adhesive hydrogel specimens. (*ii*) A pair of tweezers were pre-cooled within a -20°C refrigerator for precise placement of antifreezing hydrogels. (*iii*) During all subzero temperature tests, it is imperative to avoid any direct contact with hands, as this could result in the inadvertent thawing of the frozen hydrogels.

Antifreezing measurements

The hydrogel sheets crosslinked by different crosslinkers (i.e., MBAA, EGINA, PEG_{200}-EGINA, PEG_{400}-EGINA) were precisely sectioned using a disc-shaped mold with a diameter of 10 mm. The resulting hydrogel discs were then carefully positioned on a predetermined glass stage within a -20°C freezer. Photographs were captured at various preservation intervals, and the temperature distribution dynamics of each hydrogel were documented using an infrared thermal imager (TG165, FLIR). All statistical freezing time data, IR images and videos were meticulously recorded in triplicate. To ensure a fair comparison of the antifreezing properties, all Agar/PAAm DN hydrogels, used in antifreezing tests, were meticulously prepared with consistent and stable water contents falling within the range of 85% to 90%. This uniformity was maintained by using identical proportions of agar and acrylamide (AM) monomers, initiators, and crosslinkers across all hydrogel samples.

Characterizations

Utilizing a Bruker Avance 400 MHz NMR Spectrometer, ^{1}H-NMR spectroscopy was executed, encompassing the acquisition of 16 scans with a relaxation delay of 1 s. DSC measurements were performed using a Discovery DSC250 (TA Instruments, USA) under nitrogen flow. The small gel disc (5-10 mg) was encapsulated in a hermetic Aluminum pan and controlled heating rate of 10°C min^{-1} (Cool-Heat-Cool mode), while an empty pan was used as reference. For swelling test, all hydrogels underwent freeze-drying before being immersed in deionized water to induce swelling. The alteration in their mass was documented at various time intervals until the gel matrix attained equilibrium.

MD simulations of double-network hydrogels. Upon generating Agar/PAAm DN networks using the RWRP algorithm, the next step involved solvating these networks with TIP3P water molecules. To prevent atom collapse, we removed any water molecules within a distance of 2.4 Å from the networks. This solvated DN hydrogel model allowed for variations in water content, ranging from 50% to 90%, which closely matched the experimental conditions. Subsequently, the solvated system underwent energy minimization and equilibration through MD simulations at a temperature of 298 K using the NPT ensemble and 3D periodic boundary conditions. The MD production runs were carried out for 100 ns using the all-atom NAMD 2.12 package [34], employing the CHARMM force field [35]. The simulation ensemble was set to NVT (constant number of atoms, constant volume, and constant temperature), and 3D periodic boundary conditions were applied. To maintain the temperature at 298 K, the Langevin thermostat method was employed with a damping coefficient of 1 ps^{-1}. Covalent bonds, including hydrogen bonds, were constrained using the RATTLE method, allowing for the use of a larger timestep of 2 fs with velocity Verlet integration of Newton's motion equation. During the MD production runs, long-range electrostatic potentials were calculated using the Particle Mesh Ewald (PME) method with a grid spacing of 0.5 Å. Short-range van der Waals (VDW) potentials were estimated using a switching function with a twin-range cutoff set at 12 Å and 14 Å. To facilitate further analysis, MD trajectories were saved every 2 ps. This enabled the examination of the dynamics and behavior of the Agar/PAAm DN hydrogel system over the course of the simulation.

Declaration of Competing Interest

The authors declare no conflict of interest.

Data availability

No data was used for the research described in the article.

Acknowledgements

We thank financial supports from NSF-Polymer-2311985 and ACS-PRF-65277. Three K12 students of Keven Gong from Hudson Middle School, Alice Xu from Hudson High School, and Bowen Zheng from Copley High School were trained by this project.

Supplementary materials

Supplementary material associated with this article can be found, in the online version, at doi:10.1016/j.giant.2023.100203.

References

[1] H. Yuk, J. Wu, X. Zhao, Hydrogel interfaces for merging humans and machines, Nature Reviews Materials (2022).

[2] X. Liu, M.E. Inda, Y. Lai, T.K. Lu, X. Zhao, Engineered Living Hydrogels, Adv. Mater. 34 (26) (2022) 2201326.

[3] Q. Chen, H. Chen, L. Zhu, J. Zheng, Fundamentals of double network hydrogels, J. Materials Chemistry B 3 (18) (2015) 3654–3676.

[4] S.W. Huang, L. Hou, T.Y. Li, Y.C. Jiao, P.Y. Wu, Antifreezing Hydrogel Electrolyte with Ternary Hydrogen Bonding for High-Performance Zinc-Ion Batteries, Advanced Materials 34 (14) (2022) 2110140.

[5] K. Lei, M.J. Chen, P.S. Guo, J.J. Fang, J.B. Zhang, X. Liu, W.Y. Wang, Y.S. Li, Z.G. Hu, Y.J. Ma, H.W. Jiang, J.Q. Cui, J.H. Li, Environmentally Adaptive Polymer Hydrogels: Maintaining Wet-Soft Features in Extreme Conditions, Advanced Functional Materials (2023) 2303511.

[6] D. Zhang, Y.J. Tang, K.H. Zhang, Y.T. Xue, S.Y. Zheng, B.Y. Wu, J. Zheng, Multiscale bilayer hydrogels enabled by macrophase separation, Matter 6 (5) (2023) 1484–1502.

[7] K. Cheng, L. Zou, B. Chang, X. Liu, H. Shi, T. Li, Q. Yang, Z. Guo, C. Liu, C. Shen, Mechanically robust and conductive poly(acrylamide) nanocomposite hydrogel by the synergistic effect of vinyl hybrid silica nanoparticle and polypyrrole for human motion sensing, Advanced Composites and Hybrid Materials 5 (4) (2022) 2834–2846.

[8] L.L.C. Olijve, K. Meister, A.L. DeVries, J.G. Duman, S. Guo, H.J. Bakker, I.K. Voets, Blocking rapid ice crystal growth through nonbasal plane adsorption of antifreeze proteins, Proc Natl Acad Sci U S A 113 (14) (2016) 3740–3745.

[9] Y. Jian, S. Handschuh-Wang, J. Zhang, W. Lu, X. Zhou, T. Chen, Biomimetic anti-freezing polymeric hydrogels: keeping soft-wet materials active in cold environments, Mater. Horiz. 8 (2) (2021) 351–369.

[10] Y. Zhuo, S. Xiao, V. Håkonsen, J. He, Z. Zhang, Anti-icing Ionogel Surfaces: Inhibiting Ice Nucleation, Growth, and Adhesion, ACS Materials Letters 2 (6) (2020) 616–623.

[11] T. Li, H. Wei, Y. Zhang, T. Wan, D. Cui, S. Zhao, T. Zhang, Y. Ji, H. Algadi, Z. Guo, L. Chu, B. Cheng, Sodium alginate reinforced polyacrylamide/xanthan gum double network ionic hydrogels for stress sensing and self-powered wearable device applications, Carbohydr. Polym. 309 (2023) 120678.

[12] D. Zhou, F. Chen, J. Wang, T. Li, B. Li, J. Zhang, X. Zhou, T. Gan, S. Handschuh-Wang, X. Zhou, Tough protein organohydrogels, Journal of Materials Chemistry B 6 (45) (2018) 7366–7372.

[13] F. Chen, D. Zhou, J. Wang, T. Li, X. Zhou, T. Gan, S. Handschuh-Wang, X. Zhou, Rational Fabrication of Anti-Freezing, Non-Drying Tough Organohydrogels by One-Pot Solvent Displacement, Angew Chem Int Ed Engl 57 (22) (2018) 6568–6571.

[14] Y.Q. Liu, Q.Y. Liu, L. Zhong, C.C. Chen, Z.Y. Xu, Tough, antifreezing, and conductive double network zwitterionic-based hydrogel for flexible sensors, Chemical Engineering Journal 452 (2023) 139314.

[15] X.P. Morelle, W.R. Illeperuma, K. Tian, R. Bai, Z. Suo, J.J. Vlassak, Highly stretchable and tough hydrogels below water freezing temperature, Adv. Mater 30 (35) (2018) 1801541.

[16] X. Di, J. Li, M. Yang, Q. Zhao, G. Wu, P. Sun, Bioinspired, nucleobase-driven, highly resilient, and fast-responsive antifreeze ionic conductive hydrogels for durable pressure and strain sensors, J. Mater. Chem. A 9 (36) (2021) 20703–20713.

[17] Z. He, Z. Zhou, W. Yuan, Highly Adhesive, Stretchable, and Antifreezing Hydrogel with Excellent Mechanical Properties for Sensitive Motion Sensors and Temperature-/Humidity-Driven Actuators, ACS Appl. Mater. Interfaces 14 (33) (2022) 38205–38215.

[18] Z. Xie, H. Li, H.-Y. Mi, P.-Y. Feng, Y. Liu, X. Jing, Freezing-tolerant, widely detectable and ultra-sensitive composite organohydrogel for multiple sensing applications, J. Mater. Chem. C 9 (31) (2021) 10127–10137.

[19] T. Xu, D. Yang, S. Zhang, T. Zhao, M. Zhang, Z.-Z. Yu, Antifreezing and stretchable all-gel-state supercapacitor with enhanced capacitances established by graphene/PEDOT-polyvinyl alcohol hydrogel fibers with dual networks, Carbon 171 (2021) 201–210.

[20] Z. Zhou, C. Qian, W. Yuan, Self-healing, anti-freezing, adhesive and remoldable hydrogel sensor with ion-liquid metal dual conductivity for biomimetic skin, Compos. Sci. Technol. 203 (2021) 108608.

[21] Z. He, W. Yuan, Highly Stretchable, Adhesive Ionic Liquid-Containing Nanocomposite Hydrogel for Self-Powered Multifunctional Strain Sensors with Temperature Tolerance, ACS Appl. Mater. Interfaces 13 (44) (2021) 53055–53066.

[22] X. Sui, H. Guo, P. Chen, Y. Zhu, C. Wen, Y. Gao, J. Yang, X. Zhang, L. Zhang, Zwitterionic osmolyte-based hydrogels with antifreezing property, high conductivity, and stable flexibility at subzero temperature, Adv. Funct. Mater 30 (7) (2020) 1907986.

[23] X.-F. Zhang, X. Ma, T. Hou, K. Guo, J. Yin, Z. Wang, L. Shu, M. He, J. Yao, Inorganic salts induce thermally reversible and anti-freezing cellulose hydrogels, Angew. Chem., Int. Ed. 58 (22) (2019) 7366–7370.

[24] H. Sun, Y. Zhao, S. Jiao, C. Wang, Y. Jia, K. Dai, G. Zheng, C. Liu, P. Wan, C. Shen, Environment Tolerant Conductive Nanocomposite Organohydrogels as Flexible Strain Sensors and Power Sources for Sustainable Electronics, Adv. Funct. Mater. 31 (24) (2021) 2101696.

[25] J. Wu, Z. Wu, X. Lu, S. Han, B.-R. Yang, X. Gui, K. Tao, J. Miao, C. Liu, Ultrastretchable and stable strain sensors based on antifreezing and self-healing ionic organohydrogels for human motion monitoring, ACS Appl. Mater. Interfaces 11 (9) (2019) 9405–9414.

[26] Y. Wang, Y. Xia, P. Xiang, Y.Y. Dai, Y. Gao, H. Xu, J.A. Yu, G.H. Gao, K.X. Chen, Protein-assisted freeze-tolerant hydrogel with switchable performance toward customizable flexible sensor, Chemical Engineering Journal 428 (2022) 131171.

[27] C. Lu, J. Qiu, W. Zhao, E. Sakai, G. Zhang, R. Nobe, M. Kudo, T. Komiyama, Low-temperature adaptive conductive hydrogel based on ice structuring proteins/CaCl2 anti-freeze system as wearable strain and temperature sensor, International Journal of Biological Macromolecules 188 (2021) 534–541.

[28] Z. Zhang, X.-Y. Liu, Control of ice nucleation: freezing and antifreeze strategies, Chem. Soc. Rev 47 (18) (2018) 7116–7139.

[29] D. Zhang, Y. Liu, Y. Liu, Y. Peng, Y. Tang, L. Xiong, X. Gong, J. Zheng, A General Crosslinker Strategy to Realize Intrinsic Frozen Resistance of Hydrogels, Adv. Mater. 33 (42) (2021) 2104006.

[30] Q. Chen, L. Zhu, C. Zhao, Q. Wang, J. Zheng, A robust, one-pot synthesis of highly mechanical and recoverable double network hydrogels using thermoreversible sol-gel polysaccharide, Adv. Mater. 25 (30) (2013) 4171–4176.

[31] J.P. Gong, Y. Katsuyama, T. Kurokawa, Y. Osada, Double-network hydrogels with extremely high mechanical strength, Adv. Mater. 15 (14) (2003) 1155–1158.

[32] M. Zhang, D. Zhang, H. Chen, Y. Zhang, Y. Liu, B. Ren, J. Zheng, A multiscale polymerization framework towards network structure and fracture of double-network hydrogels, npj Computational Materials 7 (1) (2021) 39.

[33] Y. Liu, X. Liu, B. Duan, Z. Yu, T. Cheng, L. Yu, L. Liu, K. Liu, Polymer–Water Interaction Enabled Intelligent Moisture Regulation in Hydrogels, The Journal of Physical Chemistry Letters 12 (10) (2021) 2587–2592.

[34] L. Kale, R. Skeel, M. Bhandarkar, R. Brunner, A. Gursoy, N. Krawetz, J. Phillips, A. Shinozaki, K. Varadarajan, K. Schulten, NAMD2: greater scalability for parallel molecular dynamics, J. Comput. Phys. 151 (1) (1999) 283–312.

[35] A.D. MacKerell, D. Bashford, M. Bellott, R.L. Dunbrack, J.D. Evanseck, M.J. Field, S. Fischer, J. Gao, H. Guo, S. Ha, D. Joseph-McCarthy, L. Kuchnir, K. Kuczera, F.T.K. Lau, C. Mattos, S. Michnick, T. Ngo, D.T. Nguyen, B. Prodhom, W.E. Reiher, B. Roux, M. Schlenkrich, J.C. Smith, R. Stote, J. Straub, M. Watanabe, J. Wiorkiewicz-Kuczera, D. Yin, M. Karplus, All-atom empirical potential for molecular modeling and dynamics studies of proteins, J. Phys. Chem. B 102 (18) (1998) 3586–3616.